

Bio-Techne is offering Travel Grants
to IMMUNOLOGY 2015™

R&D SYSTEMS™
a biotechne brand
>Apply Now



Geranylgeranylation but Not GTP Loading Determines Rho Migratory Function in T Cells

This information is current as
of March 4, 2015.

Sonia Waiczies, Ivo Bendix, Timour Prozorovski, Maya
Ratner, Irina Nazarenko, Caspar F. Pfueller, Alexander U.
Brandt, Josephine Herz, Stefan Brocke, Oliver Ullrich and
Frauke Zipp

J Immunol 2007; 179:6024-6032; ;
doi: 10.4049/jimmunol.179.9.6024
<http://www.jimmunol.org/content/179/9/6024>

References This article **cites 36 articles**, 19 of which you can access for free at:
<http://www.jimmunol.org/content/179/9/6024.full#ref-list-1>

Subscriptions Information about subscribing to *The Journal of Immunology* is online at:
<http://jimmunol.org/subscriptions>

Permissions Submit copyright permission requests at:
<http://www.aai.org/ji/copyright.html>

Email Alerts Receive free email-alerts when new articles cite this article. Sign up at:
<http://jimmunol.org/cgi/alerts/etoc>

The Journal of Immunology is published twice each month by
The American Association of Immunologists, Inc.,
9650 Rockville Pike, Bethesda, MD 20814-3994.
Copyright © 2007 by The American Association of
Immunologists All rights reserved.
Print ISSN: 0022-1767 Online ISSN: 1550-6606.



Geranylgeranylation but Not GTP Loading Determines Rho Migratory Function in T Cells¹

Sonia Waiczies,^{2*} Ivo Bendix,^{2*} Timour Prozorovski,* Maya Ratner,[†] Irina Nazarenko,[‡] Caspar F. Pfueller,* Alexander U. Brandt,* Josephine Herz,* Stefan Brocke,[§] Oliver Ullrich,[¶] and Frauke Zipp^{3*}

Rho GTPases orchestrate signaling pathways leading to cell migration. Their function depends on GTP loading and isoprenylation by geranylgeranyl pyrophosphate (GGpp). In this study, we show that in human T cells, geranylgeranylation—and not GTP loading—is necessary for RhoA-mediated downstream events. As a result of GGpp depletion with the 3-hydroxy-3-methylglutaryl-CoA reductase inhibitor atorvastatin, RhoA was sequestered from the membrane to the cytosol and, notwithstanding increased GTP loading, the constitutive activation of its substrate Rho-associated coiled-coil protein kinase-1 was blocked. In line with this, T cells expressing increased GTP-RhoA failed to form an intact cytoskeleton and to migrate toward a chemokine gradient. In vivo treatment with atorvastatin in the rodent model of multiple sclerosis markedly decreased the capacity of activated T cells to traffic within the brain, as demonstrated by multiphoton analysis. Thus, tethering of RhoA to the membrane by GGpp is determinant for T cell migration and provides a mechanism for preventing T cell infiltration into inflamed compartments by 3-hydroxy-3-methylglutaryl-CoA reductase inhibitors, *The Journal of Immunology*, 2007, 179: 6024–6032.

Immune surveillance and specific immune responses in the CNS and other tissues are absolutely dependent on migration and invasion of T cells. During T cell migration, small GTPases of the Ras homolog (Rho) family (including Rho, Rac, and Cdc42) play an important and often crucial role by switching on effector signal cascades required for cytoskeletal organization, which then enables cell movement. They are typically responsible for the organization of actin filaments which support actomyosin contractility and cell body translocation (1, 2). During these cytoskeletal processes, RhoA recruits and activates Rho-associated coiled-coil protein kinase (ROCK1),⁴ a serine/threonine kinase consisting of functional motifs at the C terminus including a Rho-binding domain (RBD) and a pleckstrin homology domain, which under resting conditions masks the active site of the ki-

nase domain at the N terminus. After formation of the RhoA-ROCK1 complex, ROCK1 can be constitutively activated by caspase-3-mediated cleavage (3).

Small GTPases such as RhoA contain an isoprenylation site (CAAX or CXC motif) in the C terminus (4). The amino acid X for RhoA is leucine and this GTPase is prenylated by C₂₀ geranylgeranyl pyrophosphate (GGpp) (5, 6). Prenylation has been described as an essential posttranslational lipid modification for small GTPases to tether to the cytoplasmic membrane and subsequently interact with downstream effector molecules (7), whereas GTP coupling by upstream guanine nucleotide exchange factors has been assumed to be the key mechanism for the activation of these signaling molecules (8). Both modifications are important for GTPases to undertake their diverse cellular functions, including cell survival, differentiation, and migration.

One way of manipulating the functionality of small GTPases is to deplete the cellular isoprenoid pool. This may be achieved by 3-hydroxy-3-methylglutaryl-CoA (HMG-CoA) reductase inhibitors (HMGCRI), which are known to prevent de novo synthesis of isoprenoids and to have anti-inflammatory properties significantly reducing infiltration of inflammatory immune cells into the CNS (9–11). An important therapeutic strategy in the treatment of neuroinflammatory disease such as multiple sclerosis (MS) is to block entry and migration of encephalitogenic T cells into the CNS compartment because this precedes disease exacerbations (12). Although we and other groups could previously prevent immune cell infiltration into the CNS by antagonizing HMG-CoA reductase with HMGCRI (9–11), it is still not clear whether these drugs are already regulating CNS Ag-specific cells outside the brain (11, 13) or whether they are directly blocking the migration of these cells into and within the CNS.

In this study, we wanted to clarify the significance of depleting GGpp by the HMGCRI atorvastatin on Rho downstream events, specifically migration, in T cells. Surprisingly, we found increased levels of GTP-RhoA after GGpp depletion that did not however result in enhanced Rho effector signaling. In fact, while GTP-RhoA was sequestered to the cytosolic compartment following

*Cecilie-Vogt-Clinic for Molecular Neurology, Charité–University Medicine and Max Delbrück Center for Molecular Medicine, Berlin, Germany; [†]Experimental Pathology, Department of Pathology, Hadassah Medical School, Jerusalem, Israel; [‡]Institute of Pathology, Charité–University Medicine, Berlin, Germany; [§]Cellular and Molecular Pharmacology, University of Connecticut Health Center Farmington, CT 06030; and [¶]Institute of Anatomy, University of Zurich, Zurich, Switzerland

Received for publication March 23, 2007. Accepted for publication August 3, 2007.

The costs of publication of this article were defrayed in part by the payment of page charges. This article must therefore be hereby marked *advertisement* in accordance with 18 U.S.C. Section 1734 solely to indicate this fact.

¹ This work was supported by grants from Charité (to S.W.; Habilitationprojekt 2006-202a), and from the Federal Ministry of Education and Research (German Israeli Cooperation) and the German Research Foundation (Deutsche Forschungsgemeinschaft: Sonderforschungsbereich 650) to F.Z.

² S.W. and I.B. contributed equally.

³ Address correspondence and reprint requests to Dr. Frauke Zipp, Cecilie-Vogt-Clinic for Molecular Neurology, Charité–University Medicine and Max Delbrück Center for Molecular Medicine, Charitéplatz 1, 10117 Berlin, Germany. E-mail address: frauke.zipp@charite.de

⁴ Abbreviations used in this paper: ROCK1, Rho-associated coiled-coil protein kinase 1; RBD, Rho-binding domain; GGpp, geranylgeranyl pyrophosphate; HMG-CoA, 3-hydroxy-3-methylglutaryl-CoA; HMGCRI, HMG-CoA reductase inhibitor; PLP, proteolipid protein; NP40, Nonidet P40; 7-AAD, 7-aminoactinomycin D; RT, room temperature; MFI, mean fluorescence intensity; PB, peripheral blood; MLC, myosin L chain; RIPA, radioimmunoprecipitation assay.

Copyright © 2007 by The American Association of Immunologists, Inc. 0022-1767/07/\$2.00

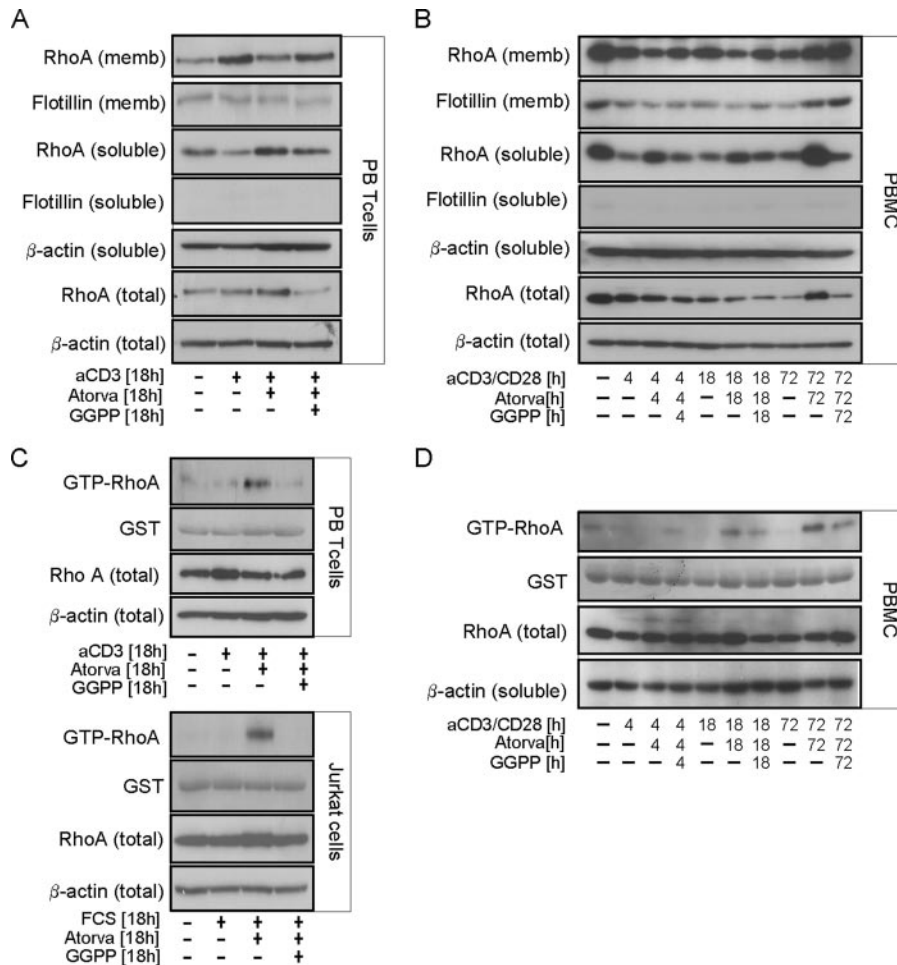


FIGURE 1. GGpp depletion causes a cytosolic sequestration and increased GTP loading of RhoA. *A*, Human peripheral CD3⁺ T cells were preincubated with or without atorvastatin (25 μ M) and GGpp (20 μ M) for 18 h and shortly (1 h) activated with anti-CD3 (as indicated). After incubation, cells were harvested and lysed. For subcellular localization of RhoA, cells were lysed and lysates were fractionated into soluble and membrane fractions by ultracentrifugation (see *Materials and Methods*). The expression of RhoA in the different compartments was analyzed by immunoblotting. As control for the subcellular fractionation, an Ab against flotillin-1 (specifically located in membrane domains) was used. *B*, PBMC were incubated with or without atorvastatin and GGpp as in *A* and in parallel with anti-CD3 and anti-CD28 for different time points (as indicated). Following harvesting, cells were lysed and lysates fractionated as in *A* and RhoA was detected in the different compartments by immunoblotting. *C*, For GTP-loading assays, peripheral CD3⁺ T cells and Jurkat cells were activated in the presence or absence of atorvastatin and GGpp for 18 h and lysed as in *A*. Clarified lysates were incubated with rhotekin RBD-GST protein bound to agarose beads (see *Materials and Methods*). The amount of RhoA that precipitated with RBD, indicative of the amount of GTP-bound RhoA, was analyzed by immunoblotting. As a loading control, shown is a Coomassie stain showing loaded GST, as well as the expression of total RhoA and β -actin in the total lysates. These experiments are representative of five separate experiments. *D*, PBMC were incubated under conditions as in *B* and after harvesting, lysates were processed as in *C*. GTP-loaded RhoA and total RhoA were detected by immunoblotting.

GGpp depletion, the constitutive activation of its specific substrate ROCK1 was strongly inhibited. In line with the latter finding, we observed a disrupted cytoskeleton in T cells following GGpp depletion and failure in their migration following both in vitro and in vivo treatment with atorvastatin. Therefore, we conclude that Rho function in migration depends on membrane localization and not GTP binding, which renders Rho isoprenylation an optimal target for prevention of T cell entry into inflamed compartments such as the CNS.

Materials and Methods

Materials

Pure atorvastatin (provided by Pfizer) was dissolved in 2% DMSO/ethanol (carrier was tested as vehicle control). Mevalonate was prepared, as already described, by activating L-mevalonic acid lactone (Sigma-Aldrich) (10). Isoprenoid intermediates (Fpp, GGpp) were obtained from Sigma-Aldrich. The GST-tagged rhotekin RBD was expressed from plasmid pGEX-2T-RBD (established by Dr. M. A. Schwartz, Scripps Research Institute, La Jolla, CA and provided by Dr. S. Offermanns, University of Heidelberg, Heidelberg, Germany).

In vivo atorvastatin treatment and induction of active experimental autoimmune encephalomyelitis

Animal experiments were conducted according to the regulations issued by the local State Office for Animal Welfare. SJL/J and C57BL/6 mice (purchased from Charles River Laboratories) were treated and immunized as previously described (10). Briefly, atorvastatin (Pfizer) was freshly dissolved in 2% DMSO before s.c. administration at a daily dose of 10 mg/kg body weight. Animals were immunized s.c. with 250 μ g of proteolipid protein peptide 139–151 (PLP_{139–151},_{140S}) (for SJL/J mice) or 250 μ g of mouse myelin oligodendrocyte glycoprotein peptide 35–55 (for C57BL/6 mice) in an emulsion consisting of CFA (Difco) and 6 mg/ml *Mycobacterium tuberculosis* H37Ra (Difco). A total of 200 ng of pertussis toxin (List Biological Laboratories) was administered i.p. at days 0 and 2.

Human and mouse T cells

PBMCs were obtained from heparinized peripheral blood (PB) of healthy donors and isolated by Ficoll Hypaque (Nycomed) density gradient centrifugation. CD3⁺ T cells were obtained by MACS technology using human CD3 microbeads and following the company's instructions (Miltenyi Biotec). Human CD4⁺ T cell lines specific for human myelin basic protein

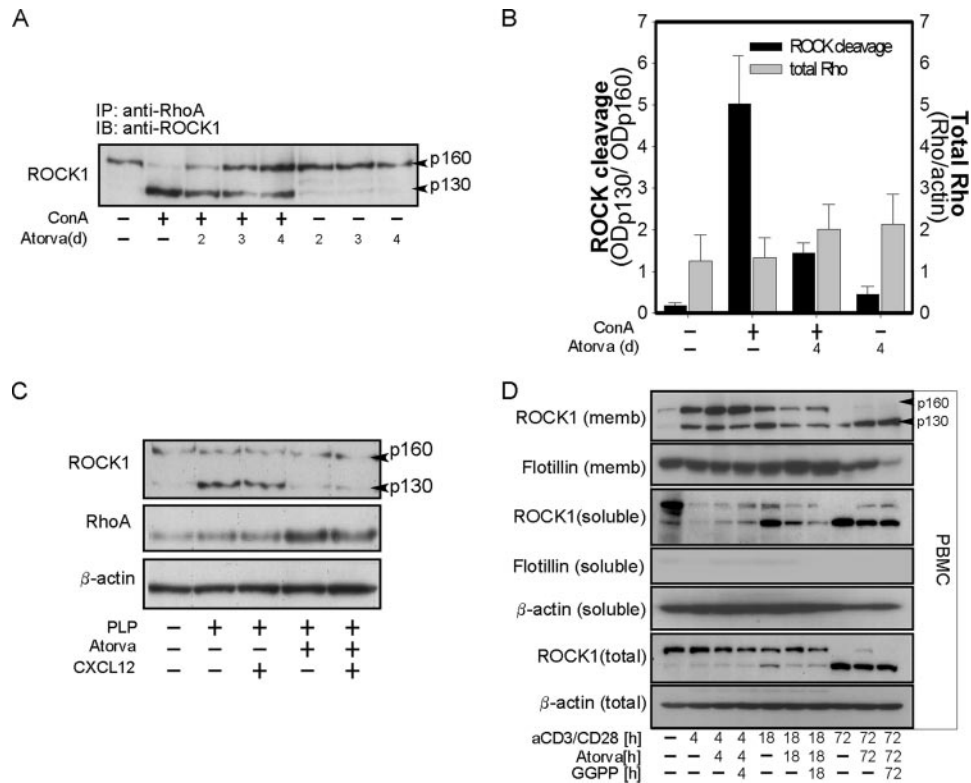


FIGURE 2. HMGCR inhibition by atorvastatin blocks constitutive activation of ROCK1 but not its association to RhoA. *A*, Human PBMC were treated with Con A and 25 μ M atorvastatin (as indicated) and then lysed in RIPA buffer (see *Materials and Methods*). RhoA was immunoprecipitated from the cleared lysates and then subjected to immunoblotting. Different forms of ROCK1 (full p160 form and cleaved p130 form) were then detected with a specific Ab against ROCK1. *B*, Cleared lysates from PBMC were subjected to immunoblotting as in *A* and the different forms of ROCK1, RhoA, and β -actin were detected with specific Abs. The extent of ROCK1 cleavage was quantified by calculating an index between the OD of the uncleaved 160-kDa form and the OD of the cleaved 130-kDa form. Shown are the mean values \pm SEM from three independent experiments (with human PBMC) of ROCK1 cleavage and levels of total RhoA (normalized to β -actin). *C*, Mouse PLP-specific CD4⁺ T cells were incubated with 25 μ M atorvastatin for 4 days and lysed. Lysates were subjected to immunoblotting and the different forms of ROCK1, RhoA, and β -actin were detected with specific Abs. Incubation with the chemoattractant CXCL12 used in the migration assays did not alter the atorvastatin-mediated inhibition of ROCK1 cleavage. *D*, PBMC were incubated with or without atorvastatin (25 μ M) and GGpp (20 μ M) and in parallel with anti-CD3 and anti-CD28 for different time points (as indicated). Following harvesting, cells were lysed and separated into soluble and membrane fractions by ultracentrifugation (see *Materials and Methods*). The expression of ROCK1 in the different compartments was analyzed by immunoblotting. As control for the subcellular fractionation, the level of flotillin-1 (specifically located in membrane domains) was analyzed.

were established using a modified “split-well” protocol, as has been previously described (14). Myelin basic protein-specific T cell lines were stimulated weekly with Ag and 10 IU/ml recombinant human IL-2 (Hoffmann-La Roche, provided by Dr. C. W. Reynolds at National Cancer Institute, Frederick, MD) was added to the cultures. Mouse CD4⁺ T cell lines recognizing PLP_{139–151,140S} were established from SJL/J mice as previously described (15). Ag specificity for both human and mouse autoantigen-specific T cell lines was tested weekly by a standard [³H]thymidine incorporation proliferation assay (14).

Caspase-3-like activity assay

For the analysis of asparagine-glutamine-valine-asparagine-7-amido-4-methylcoumarin (DEVD)-amc-cleaving caspase activity, we used a previously described protocol (16). Briefly, T cells were plated in 96-well flat-bottom microtiter plates for 24–72 h. Thereafter, T cells were incubated for 10 min in lysis buffer (60 mM NaCl, 5 mM Tris-HCl, 2.5 mM EDTA, 0.25% Nonidet P40 (NP40)) and cytosolic extracts were incubated for 30 min with 20 μ M of the fluorogenic substrate Ac-DEVD-AMC (Bachem). The level of fluorescence measured at 360 nm excitation and 480 nm emission wavelengths using a CytoFluor 2400 cytofluorometer (Millipore) is an indication of caspase-3-like activity.

Apoptosis induction and annexin/7-aminoactinomycin D (7-AAD) assay

Apoptosis was induced by incubating PBMC (5×10^6) with 30 μ M etoposide for 48 h. Cells were then washed with ice-cold PBS and resuspended in binding buffer (10 mM HEPES (pH 7.4), 140 mM NaCl, 2.5 mM CaCl₂). Thereafter, 10^5 cells were incubated with 7-AAD and PE-conju-

gated annexin V (BD Biosciences), and then analyzed by flow cytometry using a FACSCalibur flow cytometer (BD Biosciences) equipped with CellQuest software. The percentages of annexin V⁻/7-AAD⁻, annexin V⁺/7-AAD⁻, and annexin V⁺/7-AAD⁺ populations were calculated corresponding to the distribution in the set quadrants.

Migration assays

Chemotaxis experiments with human and mouse T cells were performed using transwell polycarbonate membrane Boyden chambers as previously described (17). Briefly, 600 μ l of cell culture medium (RPMI 1640, 10% FCS) with or without recombinant stromal-derived factor CXCL12 (R&D Systems) chemokine were added to 24-well plates (lower chamber) and 100 μ l of T cells (equivalent to 200,000 cells) were added to an upper chamber consisting of a transwell polycarbonate insert with 5- μ m pore size (6.5 mm diameter; Costar). The cells were then allowed to migrate at 37°C for 3 h. At the end of the experiment, the cells in the lower chamber were collected and counted by flow cytometry.

CXCR4 surface expression

Cells were stained with an Ab recognizing human CXCR4 (BD Biosciences). Measurements were performed on a FACSCalibur flow cytometer (BD Biosciences) and analyzed with CellQuest software.

Subcellular fractionation and immunoblotting

For subcellular fractionation, cells were homogenized in lysis buffer I (1 mM EDTA, 20 mM Tris-HCl (pH 7.4)) including a mixture of protease inhibitors (10 μ g/ml aprotinin, 1 mM Na₂VO₄, and 100 μ g/ml PMSF) and centrifuged at 100,000 \times g using an ultracentrifuge (OptimaMax, TL55

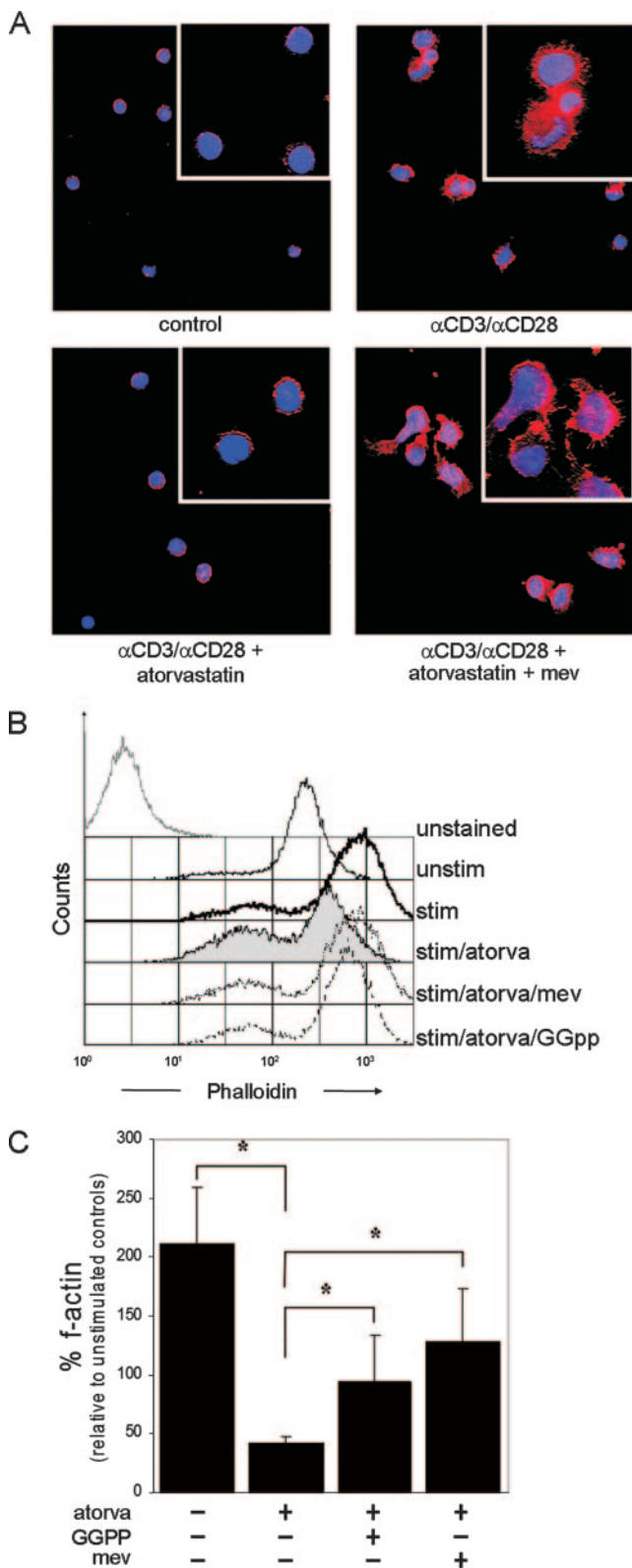


FIGURE 4. Depletion of GGpp causes disturbances in actin cytoskeletal dynamics in T cells. **A**, Human peripheral T cells were activated with anti-CD3 and anti-CD28 for 72 h and incubated with atorvastatin (25 μ M) and mevalonate (100 μ M). Cells were then stained for F-actin with rhodamine-phalloidin (red) and nuclei were stained with Hoechst 33342 (blue). Preparations were visualized by using an inverse fluorescence microscope for triple immunofluorescence. Five random fields from each section were viewed under a $\times 20$ objective ($\times 100$ in image inserts). **B**, Mouse PLP-specific CD4⁺ T cells were activated with Con A and incubated with 25 μ M atorvastatin, 100 μ M mevalonate, or 20 μ M GGpp (as indicated)

(1/1000 dilution; Amersham Pharmacia). Detection of F-actin was performed with rhodamine-coupled phalloidin (1/50 dilution; Molecular Probes). Total number of cells was analyzed by counterstaining with 1 μ g/ml Hoechst 33342 (Sigma-Aldrich) added together with secondary Ab. Preparations were visualized by using an inverse fluorescence microscope (Leica DMRA) and digitized by Leica DC Viewer 3.2, merging of images was conducted with Adobe Photoshop 5.5.

For flow cytometric analysis, we adapted a protocol from Egger et al. (18). Briefly, cells were washed with PBS and thereafter fixed with 2% PFA for 15 min at RT in dark. After thoroughly washing with PBS, cells were permeabilized with saponin buffer (0.5% saponin, 0.5% BSA) for 10 min and then resuspended in staining solution containing 50 ng/ml FITC-phalloidin (Sigma-Aldrich). After 45 min of incubation at RT in dark, cells were thoroughly washed again and mean fluorescence intensities (MFI) were measured using a FACSCalibur flow cytometer (BD Biosciences) and analyzed with CellQuest software.

Ex vivo multiphoton microscopy

Splenocytes from atorvastatin-treated and control C57BL/6 mice were activated for 72 h with anti-CD3/anti-CD28 ((1 μ g/ml; BD Biosciences) and stained with 2.5 μ M Celltracker Orange 5-(and 6)-(((4-chloromethyl)benzoyl)amino) tetramethylrhodamine (CMTMR; Invitrogen Life Technologies) for 30 min at 37°C. Acute hippocampal brain slices were prepared from p10-day-old C57BL/6 mice pups. Blood vessels were stained by intracardial perfusion with FITC-dextran (Sigma-Aldrich) directly before decapitation of pups and preparation of slices. Acute slices were placed in artificial CSF (124 mM NaCl, 1.25 mM NaH₂PO₄, 26 mM NaHCO₃, 3 mM KCl, 1.6 mM CaCl₂, 1.8 mM MgSO₄, and 10 mM glucose (pH 7.35)) aerated with carbogen (95% O₂, 5% CO₂) and were allowed to recover for at least 60 min at room temperature. After recovery, slices were mounted in a perfusion chamber and perfused constantly with carbogen-aerated artificial CSF at 35°C and either the vehicle or atorvastatin-treated cells were applied. T cell behavior was imaged over a maximum of 3 h per slice with an upright SP2 confocal microscope (Leica) equipped with a $\times 20$ water immersion objective (numerical aperture 0.5; Leica). Fluorescence dyes were excited simultaneously by a Ti:Sapphire Laser (Spectra Physics) using multiphoton excitation at a 840 nm wavelength. Fluorescence from green (FITC) and red (CMTMR) channels was collected using two external nondescanned detectors. Four-dimensional (*x-y-z* plane, *t*) images were acquired from various slice depths (50–150 μ m) every 60–120 s using Leica Confocal software. Image and cell movement analysis of multi-color three-dimensional time series was made using Velocity (Improvision) and ImageJ (W. Rasband, National Institutes of Health, Bethesda, MD) software.

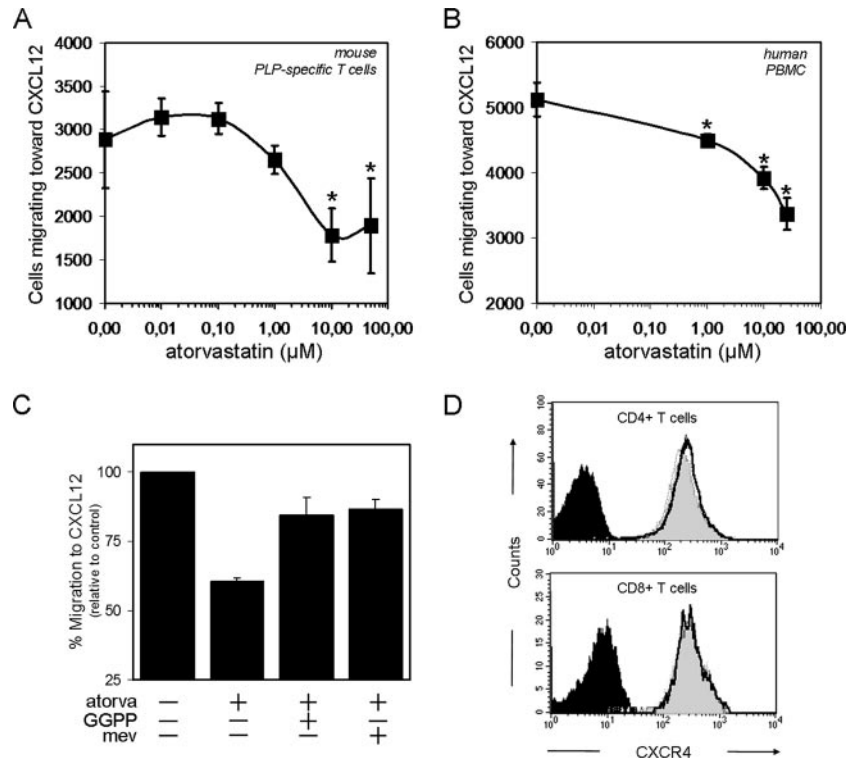
Results

Sequestration of RhoA to the T cell cytosolic compartment upon GGpp depletion

Our observation of a reduced immune cell infiltration into the CNS following therapy with the HMGCR inhibitor atorvastatin (10) led us to study here the significance of isoprenoid depletion on RhoA migratory function, specifically in activated T cells. First, we analyzed the subcellular localization (cytosolic vs membrane fractions) of this GTPase in human CD3⁺ PB T cells activated with anti-CD3, following 18 h treatment with atorvastatin. In these experiments, we observed an accumulation of RhoA in the cytosolic fraction and a decreased association of this GTPase with the plasma membrane as a consequence of GGpp depletion (Fig. 1A). A marked accumulation of RhoA was still observed in the cytosol after 72 h of atorvastatin treatment in PBMC triggered with anti-CD3 and anti-CD28 (Fig. 1B).

for 36 h. Following incubation, cells were fixed, permeabilized, and stained intracellularly for F-actin with FITC-phalloidin. MFI were measured using a FACSCalibur (BD Biosciences) and analyzed with CellQuest. **C**, The extent of actin polymerization was calculated from three independent experiments. Shown are the mean F-actin values in percent compared with unstimulated controls from the different conditions \pm SEM. Statistical analysis between the groups was done with the Mann-Whitney nonparametric test (*, *p* < 0.05).

FIGURE 5. GGpp depletion inhibits migration of T cells toward CXCL12. **A**, Mouse PLP-specific CD4⁺ T cells were incubated for 3 days with different doses of atorvastatin and then applied to a transwell system consisting of a CXCL12 chemokine gradient (see *Materials and Methods*). Cells were applied to an upper chamber and the amount of cells migrating to the lower chamber was quantified by flow cytometry. **B**, Human PBMC were incubated for 4 h with different doses of atorvastatin and applied to a transwell system as in **A**. Statistical analysis between the groups was done with the Mann-Whitney nonparametric test (*, $p < 0.05$). **C**, Incubation with intermediary downstream products of HMGCR, mevalonate, and GGpp (as indicated) prevented the inhibition of PBMC to migrate toward the CXCL12 gradient following 25 μ M atorvastatin. **D**, Parallel to the migration assays human PBMC were incubated for 4 h with 25 μ M atorvastatin, stained for immune surface markers CD4, CD8 and CD19 and for the chemokine receptor CXCR4 using specific Abs, and analyzed by flow cytometry. Shown in each histogram is the isotype control (black closed) and CXCR4 expression in untreated (gray closed) and atorvastatin-treated cells (thick black line).



Increased Rho GTP loading in T cells following GGpp depletion

Because GTP loading has been considered as a crucial step in RhoA activation and function, we next analyzed the amount of GTP-bound RhoA in the same cells shown in Fig. 1A (PB T cells) following 18 h treatment with atorvastatin. To determine the extent of GTP binding, cell lysates were incubated with the RBD of rhotekin, a substrate and effector molecule of RhoA. The amount of RhoA that precipitated with RBD is indicative of the amount of GTP-bound RhoA. Surprisingly, the amount of GTP-bound Rho increased distinctly following atorvastatin incubation in PB T cells (Fig. 1C). Importantly, the increase in GTP binding in response to atorvastatin treatment was also dependent on depletion of the isoprenoid GGpp as was the cytosolic accumulation of RhoA. This finding, which was also confirmed in Jurkat cells (Fig. 1C) and PBMC (Fig. 1D), clearly contradicts earlier observations of reduced Rho activation in myeloid (19) and lymphoma cells (20), as determined by similar GTP-binding assays. Because the latter reports applied longer incubations (at least 48 h) with HMGCR, we next performed a kinetic with atorvastatin in PBMC. We found that increased GTP binding was still evident after 72 h and this sustained GTP-Rho accumulation was also dependent on the depletion of GGpp (Fig. 1D).

Inhibition of ROCK1 cleavage despite unaltered association with RhoA following atorvastatin

Following our observations of increased RhoA GTP loading and cytosolic translocation in atorvastatin-treated T cells, we next investigated the impact on ROCK1, a specific substrate of RhoA and important effector molecule for cytoskeletal organization. For this, RhoA was immunoprecipitated and its association to ROCK1 was detected by Western blotting. As shown in Fig. 2A, incubation with atorvastatin did not prevent the association of ROCK1 with RhoA, which suggests that ROCK1 is also present in the cytosol upon isoprenoid depletion and is inaccessible to membrane proteins. In fact, constitutive activation of ROCK1, typically mediated by caspase-3 (21), was in-

hibited following atorvastatin treatment in human PBMC (Fig. 2A) and mouse PLP-specific T cells (Fig. 2C). In resting conditions, the uncleaved form (160-kDa full length) of ROCK1 was predominantly observed, whereas under activating conditions, including TCR triggering (Fig. 2, C and D), the 130-kDa cleaved form dominated. Isoprenoid depletion by atorvastatin inhibited cleavage in a time-dependent manner (Fig. 2A). ROCK1 cleavage was semiquantitatively determined for all conditions by deriving a quotient from the OD of the cleaved 130-kDa band and the OD of the uncleaved 160-kDa band. The mean ROCK1 cleavage for the various conditions from three separate experiments is given in Fig. 2B.

Because these experiments suggest that the RhoA-ROCK1 complex moves to the cytosol away from membrane-associated caspase-3 following atorvastatin treatment to prevent ROCK1 cleavage, we next investigated the intracellular location of ROCK1 under these conditions in a kinetic. Under resting conditions, ROCK1 is located in the cytosol and shortly after TCR triggering (4 h) it localizes to the membrane to presumably start the cleavage process (Fig. 2D). Already after 18 h of activation, a portion of ROCK1 (mostly in cleaved form) relocates back to the cytosol and after 72 h of activation the cleaved form of ROCK1 is more prevalent in the cytosolic compartment (Fig. 2D). Although 4 h of treatment with atorvastatin already shows an accumulation of RhoA in the cytosol (Fig. 1B), ROCK1 cleavage at this time point is not yet effected (Fig. 2D). However, after 18 h and maximally after 72 h of atorvastatin treatment, less of the cleaved form of ROCK1 returns to the cytosol. After 72 h of treatment with atorvastatin the uncleaved form of ROCK1 observed in the total lysate is predominantly in the cytosol (Fig. 2D). This indicates that decreased localization of ROCK1 to the membrane, as a consequence of accumulation of its partner RhoA in the cytosol, prevents its cleavage by membrane-associated caspase-3 and possibly downstream signaling.

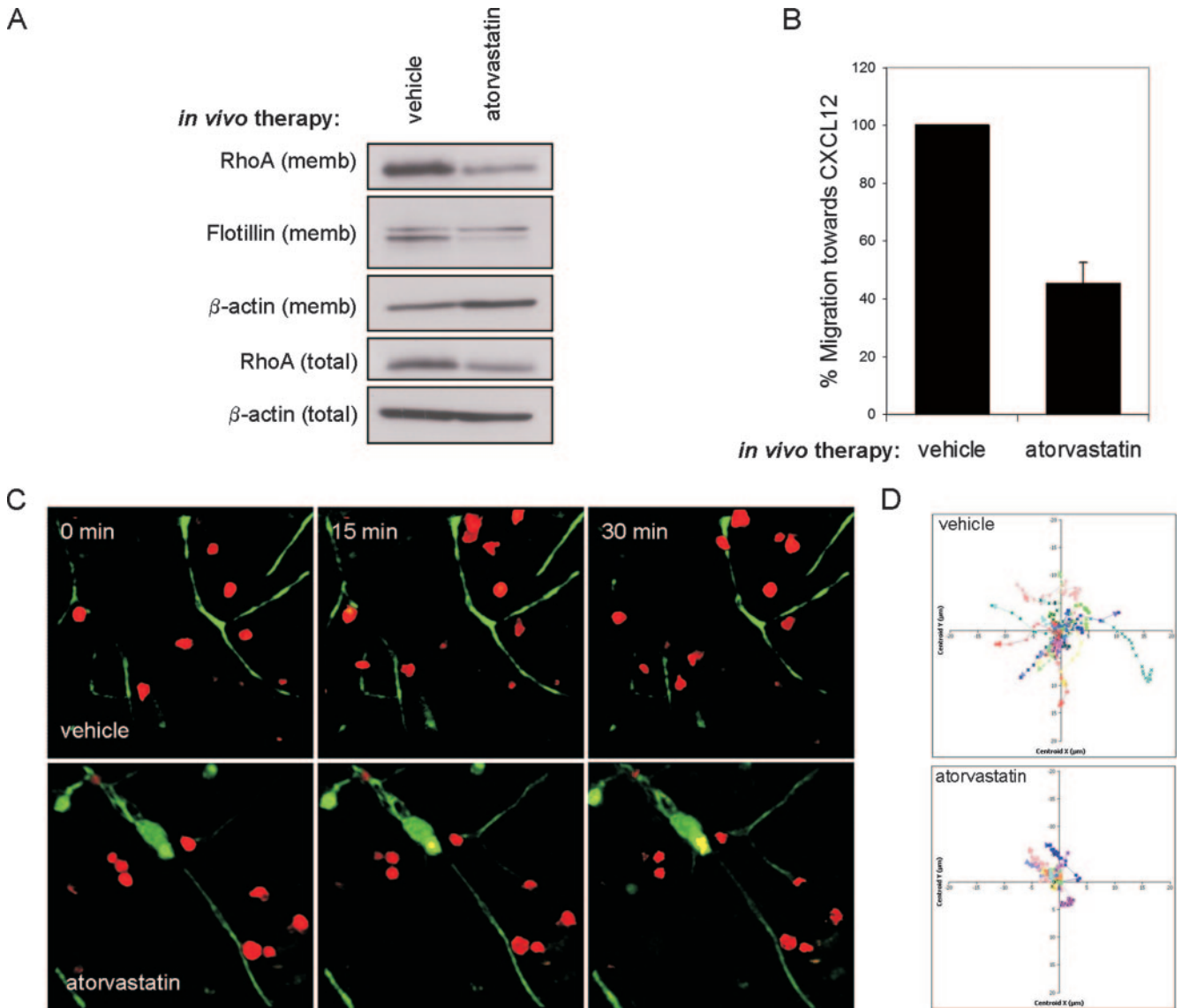


FIGURE 6. In vivo atorvastatin treatment inhibits T cell infiltration into CNS tissue. C57BL/6 mice were treated with either atorvastatin or vehicle and immunized with myelin oligodendrocyte glycoprotein peptide 35–55. *A*, Eighteen hours following the last atorvastatin or vehicle dose, mice were sacrificed; isolated splenocytes were lysed and fractionated by ultracentrifugation (see *Materials and Methods*) and expression of RhoA analyzed by immunoblotting. *B*, Following isolation of splenocytes from atorvastatin- or vehicle-treated mice, T cells were activated for 3 days with anti-CD3 and anti-CD28. Following ex vivo culture, T cells were then subjected to a CXCL12 gradient using the same transwell system used for the in vitro experiments. *C*, The same cells from the 3 day culture in *B* were applied in parallel to acute hippocampal slices from postnatal 10-day-old C57BL/6 mice pups for analysis with multiphoton microscopy. T cell behavior was imaged over a period of 3 h with a SP2 confocal microscope (Leica); shown is a representative 30-min time window. *D*, The movement behavior of atorvastatin-treated cells ($n = 18$) and vehicle-treated cells ($n = 25$) in xy direction were compared using Volocity (Improvision) software.

HMGCR inhibition by atorvastatin prevents downstream caspase-3 activation but not apoptosis

Although constitutive activation of ROCK1 is mediated by caspase-3, ROCK1 activation itself is necessary for the activation of caspase-3, via a positive feedback regulatory loop (22, 23). Furthermore, caspase-3-mediated cleavage of ROCK1 induces phosphorylation of myosin L chain (MLC) (21), a specific downstream substrate of ROCK1 (24). Thus, we next looked at downstream signaling of ROCK1 cleavage following GGpp depletion, specifically caspase-3 activation and MLC phosphorylation. As shown in Fig. 3A, in parallel to inhibition of ROCK1 cleavage (at 72 h), treatment with atorvastatin results in inhibited TCR-mediated caspase-3 activation as detected by an Ab which recognizes the cleaved, active products p19/p17 and in inhibited MLC phosphorylation. A dose-dependent inhibition of caspase-3 activity follow-

ing 72 h of HMGCR inhibition by atorvastatin was also observed by measuring cleavage of a fluorogenic substrate (Fig. 3B).

Because the above events occur in cells undergoing membrane blebbing, an essential step before apoptosis (21, 25), we wanted to know whether isoprenoid depletion by atorvastatin ultimately renders cells less susceptible toward apoptosis. To test this, we induced apoptosis with etoposide in PBMC. Atorvastatin did not render these cells resistant toward etoposide-induced apoptosis (Fig. 3C). Following a 3-day culture of PBMC with Con A, caspase-3 was also not present in the nucleus (Fig. 3D), where it is known to orchestrate DNA fragmentation during apoptosis (26), but rather colocalized with polymerized actin in the membrane/cytoplasmic compartment (Fig. 3D). Thus, atorvastatin prevents caspase-3-mediated ROCK1 cleavage and caspase-3 activity without rendering cells resistant to apoptosis.

T cell cytoskeleton is disrupted following GGpp depletion

Because the proteolytic activation of ROCK1 by caspases is critical for controlling cell cytoskeletal dynamics, we next investigated the capacity of T cells to polymerize actin following treatment with atorvastatin. For this, we stained T cells with rhodamine-coupled phalloidin, a highly specific F-actin-binding toxin which enables the measurement of changes in the level of actin polymerization. As depicted in Fig. 4A, peripheral T cells presented detectable membrane protrusions following 72 h of TCR activation with anti-CD3 and anti-CD28, thereby accumulating polymerized actin at the edge of these protrusions. Atorvastatin-treated T cells in contrast had a small round shape, failed to produce the elongated structures typical of activated T cells, and polymerized less globular actin into F-actin compared with activated cell controls. As with the regulation of Rho recruitment and ROCK1 activity, regulation of actin cytoskeletal dynamics by atorvastatin was clearly shown to be dependent on isoprenoid depletion.

To quantify these observations in actin polymerization, we adapted a previous protocol for phalloidin staining for flow cytometry (see *Materials and Methods*). PLP-specific T cells, stimulated for 36 h with Con A, were fixed, permeabilized, and stained intracellularly with FITC-coupled phalloidin. Fluorescence was measured by gating on the living lymphocyte population. As shown in Fig. 4B, atorvastatin-treated cells (shaded gray histogram) polymerize less actin as compared with activated controls (thick line open histogram) as shown by less phalloidin staining. We could also show that the ability of atorvastatin to disrupt actin cytoskeletal dynamics was dependent on depletion of mevalonate (gray line open histogram) and isoprenoid intermediates, specifically GGpp (perforated gray line histogram). Fig. 4C demonstrates the average of three separate experiments measuring the MFI of phalloidin staining in the different conditions depicted in Fig. 4B. Therefore, we could demonstrate that T cell cytoskeleton is severely disrupted following atorvastatin treatment.

Atorvastatin treatment inhibits T cell migration in the brain

Cell cytoskeletal dynamics is of vital importance for cell migration, a crucial and essential function required for immune surveillance and recruitment to the site of inflammation or damage after injury. To determine the direct influence of isoprenoid depletion by atorvastatin on the capacity of T cells to migrate, we first analyzed the responsiveness of PLP-specific T cells to CXCL12 (stromal-derived factor-1a), a potent chemoattractant for T cell migration (27). Using a transwell system, we observed a dose-dependent inhibition in the migratory capacity of mouse PLP-specific T cells after treatment for 3 days with atorvastatin (Fig. 5A) as well as of human PBMC treated with atorvastatin for 4 h (Fig. 5B). Inhibition of T cell migration by atorvastatin was clearly dependent on isoprenoid deprivation, specifically GGpp (Fig. 5C). To exclude the possibility of a direct regulation of the receptor for CXCL12 by HMGCR1, CXCR4 expression was monitored in parallel to the migration assays. As shown in Fig. 5D, we observed no regulation of CXCR4 by atorvastatin in different lymphocyte subpopulations.

To determine the *in vivo* significance of GGpp depletion on T cell migration, we analyzed the migratory properties of T cells isolated from atorvastatin-treated and vehicle-treated C57BL/6 mice. Mice from both groups were sacrificed 18 h following the last dose of atorvastatin. Similar to the *in vitro* experiments and in line with a previous study (28), less RhoA associated with the plasma membrane of cells from the atorvastatin group (Fig. 6A). We applied activated T cells from both groups to the transwell setup described above and to living brain cultures in which we analyzed migration by multiphoton microscopy, as described previously (29). Cell viability was similar for both groups. Using the transwell system, we observed a significant

reduction (55.5%) in the migration of activated T cells from atorvastatin-treated mice toward the CXCL12 gradient as compared with T cells from vehicle-treated control mice (Fig. 6B). Unlike the vehicle-treated cells (supplemental video 1),⁵ which penetrate brain tissue instantly and are then moving around, cells from atorvastatin-treated animals (supplemental video 2) were barely able to migrate into deeper regions of living brain cultures (Fig. 6C) and remained mostly stationary during the observation period of 3 h (Fig. 6D). The mean velocity of atorvastatin-treated cells during the observation was 0.006 $\mu\text{m/s}$, whereas mean velocity of vehicle-treated cells was 0.014 $\mu\text{m/s}$.

Discussion

Our current knowledge on GTPases is that these signaling molecules need to tether to the cytoplasmic membrane to interact with downstream effector molecules, and this they can do by undergoing a series of posttranslational lipid modifications including isoprenylation (7). In this study, we show that in T cells, depletion of the isoprenoid GGpp by inhibition of the HMGCR pathway impairs the recruitment of the small GTPase RhoA to the membrane but increases its GTP loading. Accumulation of RhoA in the cytosol following inhibition of HMGCR has been reported in other cell types including endothelial cells and neurons (30, 31). However, thus far, it has been assumed that as a result of isoprenylation inhibition, HMGCR1 block the activity of GTPases including RhoA by inhibiting their GTP loading (19, 20). Yet, an increased GTP loading of small GTPases has been recently associated with decreased GTPase function in CNS myeloid cells, as shown by decreased phagocytosis following treatment with inhibitors of HMGCR and geranylgeranyl transferases (32). Similar to our present report, the latter studies have also included shorter incubation times than those previously reporting a decrease in GTP loading following HMGCR1 (19, 20). However, in additional experiments, we showed that longer incubation with the HMGCR1 atorvastatin also results in a strong GTP-Rho signal. An explanation for the GTP loading following HMGCR1 is that inhibition of isoprenylation prevents the interaction of GTPases not only with the membrane but also with their negative regulator proteins, guanine nucleotide dissociation inhibitors (32), which sequester GTPases to the cytosol and prevent the release of GDP (33).

Most of the observations reported to date on the influence of isoprenoid depletion on GTPase activity have focused primarily on the GTP-binding capacity of these signaling molecules. Because we observed an increase in RhoA GTP binding, we wanted to clarify whether this is of consequence to RhoA effector function, particularly to migration. On looking into the *in vivo* association of RhoA with its specific effector kinase ROCK1 in T cells, we observed that RhoA was bound at all times to ROCK1, independent of GTP loading or cellular localization. Importantly the sequestration of RhoA to the cytosol following isoprenoid depletion should accordingly imply that ROCK1, complexed to RhoA, is no longer in close proximity to membrane-associated caspase-3 which cleaves ROCK1 into a constitutively active form (21). Indeed, isoprenoid depletion by the HMGCR1 atorvastatin not only sequestered RhoA to the cytosol but also inhibited the constitutive activation of its substrate ROCK1 in T cells. Inhibition of ROCK activation by HMGCR1 has been recently reported in embryonic stem cells (34).

Although cellular events requiring extensive cytoskeletal alterations including apoptosis have been shown to be controlled by ROCK1 cleavage, by inhibiting ROCK1 cleavage with atorvastatin we could rule out the possibility of altering the susceptibility of T cells to undergo apoptosis. Our data rather emphasize a role for ROCK1

⁵ The online version of this article contains supplemental material.

cleavage in the regulation of T cell structural rearrangements involved during cell movement, such as those required during migration. In fact, in parallel to preventing ROCK1 cleavage atorvastatin inhibited the polymerization of actin in activated T cells. The incomplete recovery in actin polymerization after addition of isoprenoids, as also observed with such substrates of ROCK1 as caspase-3, is presumably due to the influence of upstream mechanisms functioning independently of isoprenylation. Of note, atorvastatin also prevented the migration and movement of T cells into and within the brain. Similar observations have been observed in the mouse model of MS following inhibition of GG transferase GGTase-I, an enzyme required for attachment of GGpp to RhoA; less immune cells recruited into the CNS and disease was ameliorated (35). In contrast, a recent study by Ifergan et al. (36) showed that the HMGCR1 simvastatin and lovastatin do not inhibit the migration of immune cells from healthy donors, as opposed to those from MS patients; after HMGCR1 treatment, migration of cells from MS patients actually normalizes to levels observed in healthy individuals. It would be interesting to see whether the minimum threshold concentration of atorvastatin required to deplete GGpp in T cells is different between healthy individuals and MS patients. This would be of particular significance for patient clinical studies to consider both physiological differences in MS patients as well as molecular differences between HMGCR1.

In conclusion, the mechanism involved in disrupting T cell cytoskeletal dynamics and migration following inhibition of the HMGCR pathway requires two steps: while GGpp depletion sequesters GTP-bound RhoA to the cytosolic compartment and increases GTP loading, the cleavage of ROCK1 is disabled because it is kept associated to RhoA in the cytosol, thus making it inaccessible to the cleaving caspases in the membrane. The physiological significance of these signaling events is highlighted by the observation that in vivo depletion of GGpp gives rise to altered T cells, which fail to penetrate and traffic within CNS tissue. Manipulation of Rho geranylgeranylation by inhibitors of HMGCR or geranylgeranyl transferases thereby provides a therapeutic target for the direct prevention of T cell infiltration into the CNS in neuroinflammatory disease. Although therapeutic efficacy of isoprenoid depletion has so far been associated with mechanisms of immune regulation outside the brain (28), the present study also provides compelling evidence for direct control of T cell trafficking in this target organ.

Acknowledgments

We thank Nancy Nowakowski and Bibiane Seeger for technical support.

Disclosures

The authors have no financial conflict of interest.

References

- Bishop, A. L., and A. Hall. 2000. Rho GTPases and their effector proteins. *Biochem. J.* 348(Pt. 2): 241–255.
- Ridley, A. J. 2001. Rho GTPases and cell migration. *J. Cell. Sci.* 114: 2713–2722.
- Riento, K., and A. J. Ridley. 2003. Rocks: multifunctional kinases in cell behaviour. *Nat. Rev. Mol. Cell. Biol.* 4: 446–456.
- Zhang, F. L., and P. J. Casey. 1996. Protein prenylation: molecular mechanisms and functional consequences. *Annu. Rev. Biochem.* 65: 241–269.
- Adamson, P., C. J. Marshall, A. Hall, and P. A. Tilbrook. 1992. Post-translational modifications of p21rho proteins. *J. Biol. Chem.* 267: 20033–20038.
- Katayama, M., M. Kawata, Y. Yoshida, H. Horiuchi, T. Yamamoto, Y. Matsuura, and Y. Takai. 1991. The posttranslationally modified C-terminal structure of bovine aortic smooth muscle rhoA p21. *J. Biol. Chem.* 266: 12639–12645.
- Glomset, J. A., and C. C. Farnsworth. 1994. Role of protein modification reactions in programming interactions between ras-related GTPases and cell membranes. *Annu. Rev. Cell. Biol.* 10: 181–205.
- Cantrell, D. A. 2003. GTPases and T cell activation. *Immunol. Rev.* 192: 122–130.
- Nath, N., S. Giri, R. Prasad, A. K. Singh, and I. Singh. 2004. Potential targets of 3-hydroxy-3-methylglutaryl coenzyme A reductase inhibitor for multiple sclerosis therapy. *J. Immunol.* 172: 1273–1286.
- Aktas, O., S. Waiczies, A. Smorodchenko, J. Dorr, B. Seeger, T. Prozorovski, S. Sallach, M. Endres, S. Brocke, R. Nitsch, and F. Zipp. 2003. Treatment of relapsing paralysis in experimental encephalomyelitis by targeting Th1 cells through atorvastatin. *J. Exp. Med.* 197: 725–733.
- Youssef, S., O. Stuve, J. C. Patarroyo, P. J. Ruiz, J. L. Radosevich, E. M. Hur, M. Bravo, D. J. Mitchell, R. A. Sobel, L. Steinman, and S. S. Zamvil. 2002. The HMG-CoA reductase inhibitor, atorvastatin, promotes a Th2 bias and reverses paralysis in central nervous system autoimmune disease. *Nature* 420: 78–84.
- Muraro, P. A., K. P. Wandinger, B. Bielekova, B. Gran, A. Marques, U. Utz, H. F. McFarland, S. Jacobson, and R. Martin. 2003. Molecular tracking of antigen-specific T cell clones in neurological immune-mediated disorders. *Brain* 126: 20–31.
- Waiczies, S., T. Prozorovski, C. Infante-Duarte, A. Hahner, O. Aktas, O. Ullrich, and F. Zipp. 2005. Atorvastatin induces T cell anergy via phosphorylation of ERK1. *J. Immunol.* 174: 5630–5635.
- Lunemann, J. D., S. Waiczies, S. Ehrlich, U. Wendling, B. Seeger, T. Kamradt, and F. Zipp. 2002. Death ligand TRAIL induces no apoptosis but inhibits activation of human (auto)antigen-specific T cells. *J. Immunol.* 168: 4881–4888.
- Brocke, S., L. Quigley, H. F. McFarland, and L. Steinman. 1996. Isolation and characterization of autoreactive T cells in experimental autoimmune encephalomyelitis of the mouse. *Methods Enzymol.* 9: 458–462.
- Waiczies, S., A. Weber, J. D. Lunemann, O. Aktas, R. Zschenderlein, and F. Zipp. 2002. Elevated Bcl-x_L levels correlate with T cell survival in multiple sclerosis. *J. Neuroimmunol.* 126: 213–220.
- Beider, K., A. Nagler, O. Wald, S. Franitz, M. Dagan-Berger, H. Wald, H. Giladi, S. Brocke, J. Hanna, O. Mandelboim, et al. 2003. Involvement of CXCR4 and IL-2 in the homing and retention of human NK and NK T cells to the bone marrow and spleen of NOD/SCID mice. *Blood* 102: 1951–1958.
- Egger, G., A. Burda, and A. Glasner. 2001. A simple method for measuring the F-actin content of human polymorphonuclear leukocytes in whole blood. *Virchows Arch.* 438: 394–397.
- Ishibashi, T., K. Nagata, H. Ohkawara, T. Sakamoto, K. Yokoyama, J. Shindo, K. Sugimoto, S. Sakurada, Y. Takuwa, T. Teramoto, and Y. Maruyama. 2002. Inhibition of Rho/Rho-kinase signaling downregulates plasminogen activator inhibitor-1 synthesis in cultured human monocytes. *Biochim. Biophys. Acta* 1590: 123–130.
- del Real, G., S. Jimenez-Baranda, E. Mira, R. A. Lacalle, P. Lucas, C. Gomez-Mouton, M. Alegret, J. M. Pena, M. Rodriguez-Zapata, M. Alvarez-Mon, et al. 2004. Statins inhibit HIV-1 infection by down-regulating Rho activity. *J. Exp. Med.* 200: 541–547.
- Sebbagh, M., C. Renvoize, J. Hamelin, N. Riche, J. Bertoglio, and J. Breard. 2001. Caspase-3-mediated cleavage of ROCK I induces MLC phosphorylation and apoptotic membrane blebbing. *Nat. Cell. Biol.* 3: 346–352.
- Minambres, R., R. M. Guasch, A. Perez-Arago, and C. Guerri. 2006. The RhoA/ROCK-1/MLC pathway is involved in the ethanol-induced apoptosis by anoikis in astrocytes. *J. Cell. Sci.* 119: 271–282.
- Chang, J., M. Xie, V. R. Shah, M. D. Schneider, M. L. Entman, L. Wei, and R. J. Schwartz. 2006. Activation of Rho-associated coiled-coil protein kinase 1 (ROCK-1) by caspase-3 cleavage plays an essential role in cardiac myocyte apoptosis. *Proc. Natl. Acad. Sci. USA* 103: 14495–14500.
- Amano, M., M. Ito, K. Kimura, Y. Fukata, K. Chihara, T. Nakano, Y. Matsuura, and K. Kaibuchi. 1996. Phosphorylation and activation of myosin by Rho-associated kinase (Rho-kinase). *J. Biol. Chem.* 271: 20246–20249.
- Thornberry, N. A., and Y. Lazebnik. 1998. Caspases: enemies within. *Science* 281: 1312–1316.
- Faleiro, L., and Y. Lazebnik. 2000. Caspases disrupt the nuclear-cytoplasmic barrier. *J. Cell. Biol.* 151: 951–959.
- Bleul, C. C., R. C. Fuhlbrigge, J. M. Casasnovas, A. Aiuti, and T. A. Springer. 1996. A highly efficacious lymphocyte chemoattractant, stromal cell-derived factor 1 (SDF-1). *J. Exp. Med.* 184: 1101–1109.
- Dunn, S. E., S. Youssef, M. J. Goldstein, T. Prod'homme, M. S. Weber, S. S. Zamvil, and L. Steinman. 2006. Isoprenoids determine Th1/Th2 fate in pathogenic T cells, providing a mechanism of modulation of autoimmunity by atorvastatin. *J. Exp. Med.* 203: 401–412.
- Nitsch, R., E. E. Pohl, A. Smorodchenko, C. Infante-Duarte, O. Aktas, and F. Zipp. 2004. Direct impact of T cells on neurons revealed by two-photon microscopy in living brain tissue. *J. Neurosci.* 24: 2458–2464.
- Liao, J. K., and U. Laufs. 2005. Pleiotropic effects of statins. *Annu. Rev. Pharmacol. Toxicol.* 45: 89–118.
- Zipp, F., S. Waiczies, O. Aktas, O. Neuhaus, B. Hemmer, B. Schraven, R. Nitsch, and H. P. Hartung. 2007. Impact of HMG-CoA reductase inhibition on brain pathology. *Trends Pharmacol. Sci.* 28: 342–349.
- Cordle, A., J. Koenigsnecht-Talbo, B. Wilkinson, A. Limpert, and G. Landreth. 2005. Mechanisms of statin-mediated inhibition of small G-protein function. *J. Biol. Chem.* 280: 34202–34209.
- Olofsson, B. 1999. Rho guanine dissociation inhibitors: pivotal molecules in cellular signalling. *Cell. Signal.* 11: 545–554.
- Lee, M. H., Y. S. Cho, and Y. M. Han. 2007. Simvastatin suppresses self-renewal of mouse embryonic stem cells by inhibiting RhoA geranylgeranylation. *Stem Cells* 25: 1654–1663.
- Walters, C. E., G. Pryce, D. J. Hankey, S. M. Sefti, A. D. Hamilton, D. Baker, J. Greenwood, and P. Adamson. 2002. Inhibition of Rho GTPases with protein prenyltransferase inhibitors prevents leukocyte recruitment to the central nervous system and attenuates clinical signs of disease in an animal model of multiple sclerosis. *J. Immunol.* 168: 4087–4094.
- Ifergan, I., K. Wosik, R. Cayrol, H. Kebir, C. Auger, M. Bernard, A. Bouthillier, R. Moudjjan, P. Duquette, and A. Prat. 2006. Statins reduce human blood-brain barrier permeability and restrict leukocyte migration: relevance to multiple sclerosis. *Ann. Neurol.* 60: 45–55.